Research Article

Academic Platform Journal of Engineering and Smart Systems (APJESS) 14(2), 140-149, 2026

https://dergipark.org.tr/en/pub/apjess

Received: 08-12-2025, Accepted: 01-05-2026

https://doi.org/10.21541/apjess.1838629

Conformable Fractional-order Analysis of King Cobra Chaotic System and ADRC-Based Synchronization Design

[*1,2] Haris ÇALGAN

[*1] Corresponding Author, Department of Electrical-Electronics Engineering, Balıkesir University, Türkiye, haris.calgan@balikesir.edu.tr

[2] Mechatronics Research Group, Faculty of Engineering and Sciences, University of Southampton, UK

Abstract

This paper investigates the conformable fractional-order King Cobra chaotic system and proposes a robust synchronization scheme based on multi-state Proportional–Integral Active Disturbance Rejection Control (PI-ADRC). The conformable fractional derivative is introduced to generalize the classical King Cobra model which offers a simple and numerically efficient way to capture fractional-order dynamics. A detailed parametric study is carried out to explore how the fractional order and system parameters affect the onset of chaos, supported by phase portraits, Lyapunov exponents, and bifurcation analyses. To synchronize two identical chaotic systems with different initial conditions, a multi-state PI-ADRC controller equipped with an Extended State Observer (ESO) is developed. The ESO estimates and compensates for internal uncertainties and external disturbances and, allows the controller to maintain stability and accuracy even under stochastic noise. Numerical simulations show that an efficient synchronization is achieved in about one second, with smooth control signals and minimal error. The results demonstrate that the proposed approach provides a practical and robust framework for the control and synchronization of chaotic systems with conformable fractional-order behavior.

Keywords: Chaos, Conformable Fractional-order, Bifurcation, Synchronization

1. INTRODUCTION

Chaotic systems have attracted extensive research interest over the past decades due to their sensitive dependence on initial conditions, complex nonlinear dynamics, and wide applicability in engineering, physics, and secure communications [1]. Since the early discovery of chaotic attractors in classical systems such as Lorenz [2] and Chen [3], numerous models have been developed to study new types of chaotic behavior [4], [5].

In recent years, the state-of-the-art in fractional-order chaotic systems has significantly evolved with the introduction of conformable derivatives, which provide a simpler and computationally efficient framework compared to classical definitions such as Riemann–Liouville and Caputo definitions [6], [7], [8]. Recent studies have demonstrated that conformable fractional models can successfully capture complex nonlinear dynamics while maintaining compatibility with conventional numerical techniques [9]. Building on this advantage, many researchers have revisited well-known chaotic systems such as Lorenz and Chen within the conformable fractional framework, revealing new dynamical behaviors and improved controllability [10], [11], [12]. Despite these advances, the conformable fractional-order King Cobra chaotic system has received little attention [13]. In particular, its parametric sensitivity, bifurcation structure, and synchronization dynamics have not yet been systematically explored.

Previous studies on the synchronization of fractional-order chaotic systems have largely employed techniques such as adaptive control, sliding mode control, and active control [14], [15], [16], [17]. While these methods have shown effectiveness under ideal conditions, they typically rely on accurate mathematical models and careful parameter tuning. Such requirements make their practical implementation challenging, particularly in the presence of modeling uncertainties and external disturbances. In contrast, the ADRC framework has emerged as a powerful alternative due to its model-independent nature and ability to actively estimate and compensate for total disturbances in real time through an ESO [18]. Introduced by Han in 1998, ADRC has demonstrated remarkable robustness and adaptability when applied to highly nonlinear and uncertain systems [19]. More recently, researchers have extended this concept to fractional-order and conformable domains, achieving improved disturbance rejection and dynamic performance [20]. However, the integration of ADRC with

Creative Commons Attribution (CC BY) license (http://creativecommons.org/licenses/by/4.0/)

conformable fractional-order chaotic systems, particularly the King Cobra model, has not yet been thoroughly explored.

Motivated by these observations, this study focuses on the parametric analysis of the conformable fractional-order King Cobra chaotic system and proposes a multi-state PI-ADRC strategy to achieve its synchronization. The key contributions of this work can be outlined as follows. First, the classical King Cobra system is reformulated using conformable fractional derivatives which allow a detailed investigation of its nonlinear dynamics through phase portraits, bifurcation analysis, and Lyapunov exponents. Second, a multi-state PI-ADRC synchronization framework is developed, where each system state is individually controlled by a PI-based ADRC loop integrated with an ESO for real-time disturbance estimation. The robustness of the controller is further evaluated under stochastic perturbations, modeled as additive Gaussian noise in the slave dynamics, confirming its strong disturbance rejection capability and synchronization precision. Finally, extensive numerical simulations are carried out to validate the effectiveness of the proposed approach, demonstrating fast convergence, smooth control actions, and accurate state estimation across all system states.

The rest of the paper is structured as follows. Section 2 introduces the conformable fractional-order King Cobra chaotic system, provides the definition of the conformable derivative, and explains its numerical formulation. Section 3 describes the synchronization problem and outlines the design of the proposed multi-state PI-ADRC controller together with the Extended State Observer (ESO). Section 4 presents and discusses the numerical simulation results which highlight the synchronization accuracy and the controller's robustness against noise and disturbances. Finally, Section 5 concludes the study and suggests several directions for future research.

2. CONFORMABLE FRACTIONAL-ORDER KING COBRA CHAOTIC SYSTEM

It becomes possible to capture a broader spectrum of dynamic behaviors variations by introducing the conformable fractional derivative into the King Cobra chaotic system. This section presents the formulation of the conformable fractional-order King Cobra system and contains a brief overview of the conformable derivative concept, its application to the classical King Cobra model, and concludes with numerical investigations that highlight the influence of fractional parameters on chaotic flows.

2.1. Brief Definition of Conformable Fractional Derivative

Fractional calculus provides an extended framework for modeling complex dynamical phenomena characterized by memory and hereditary effects. Among the various definitions of fractional derivatives, the conformable fractional derivative has recently gained popularity due to its simplicity and compatibility with classical differentiation rules. Let $f:[0,\infty)\to\mathbb{R}$ be a differentiable function. The conformable fractional derivative of order $\alpha\in(0,1]$ is defined as [21]:

$$T_\alpha(f(t))=\lim_{\epsilon}\frac{f(t+\epsilon t^{1-\alpha})}{\epsilon},t>0. \tag{1}$$

where $T_\alpha$stands for the conformable derivative and $\alpha$is the fractional order. If f is differentiable in the classical sense, the above expression simplifies to [21]:

$$T_\alpha f(t)=t^{1-\alpha}\frac{df(t)}{dt} \tag{2}$$

This property ensures that the conformable derivative maintains linearity, product, and chain rules. Moreover, when $\alpha=1$, it naturally reduces to the standard first-order derivative, thereby preserving consistency with classical calculus.

2.2. Application to King Cobra Chaotic System

The King Cobra chaotic system, first introduced as a novel fractional-order three-dimensional nonlinear dynamical model, exhibits rich bifurcation structure [22]. The standard integer-order form can be expressed as:

$$\begin{aligned}\dot{x}&=a(y-x)+byz^2\\ \dot{y}&=cx+dxz^2\\ \dot{z}&=hz+k|x|\end{aligned} \tag{3}$$

where a,b,c,d,h and $k$are system parameters determining the system's nonlinear characteristics. To extend this model into the conformable fractional domain, each time derivative is replaced by a conformable derivative of order $\alpha_i\in(0,1]$, yielding:

$$\begin{aligned}T_{\alpha_1}x&=a(y-x)+byz^2\\ T_{\alpha_2}y&=cx+dxz^2\\ T_{\alpha_3}z&=hz+k|x|\end{aligned} \tag{4}$$

where $\alpha_1,\alpha_2,\alpha_3$denote the fractional orders correspond to each state variable. By substituting the conformable definition $T_\alpha(f)(t)=t^{1-\alpha}f'(t)$, the system can be rewritten in an equivalent differential form suitable for numerical simulation:

$$\begin{aligned}\dot{x}&=t^{\alpha_1-1}(a(y-x)+byz^2)\\ \dot{y}&=t^{\alpha_2-1}(cx+dxz^2)\\ \dot{z}&=t^{\alpha_3-1}(hz+k|x|)\end{aligned} \tag{5}$$

This formulation enables parametric exploration of the fractional orders and their effects on system stability, attractor shape, and chaotic intensity.

2.3. Numerical Investigations

Numerical simulations play a critical role in analyzing the fractional-order King Cobra system due to the complexity of its analytical solutions. The conformable fractional-order King Cobra system is numerically solved using a modified Euler-type integration method adapted for conformable

derivatives. In this approach, the conformable operator $T_{\alpha_i}(f_i) = t^{1-\alpha_i}\dot{f}_i$ is implemented through a time-weighted scaling factor t^{α_i-1} within each iteration step. This technique maintains the computational efficiency of the classical Euler method while accurately capturing the effects of fractional-order dynamics. Simulations are performed for commensurate fractional orders $\alpha = \alpha_1 = \alpha_2 = \alpha_3$ and parameter sets a, b, c, d, h, k, chosen as (8, 1, 5, -1, -5 and -6). Phase portraits in the (x, y), (y, z) and (x, z) planes are plotted to reveal transitions from periodic to chaotic behavior. The Lyapunov exponents are computed to confirm the existence of chaos, and bifurcation diagrams are generated to study parameter sensitivity.

To generate the bifurcation diagrams, a parameter sweep approach was employed. The selected bifurcation parameter (either the system parameter a or the fractional order α) was varied within the specified range using small incremental steps. For each parameter value, the conformable fractional-order system was numerically integrated using the modified Euler scheme. To eliminate transient dynamics, the first portion of the simulation data was discarded, and only the steady-state values of the state variable $y$were recorded. These steady-state samples were then plotted against the corresponding parameter values to construct the bifurcation diagrams.

For the integer-order case ($\alpha = 1$), the conformable fractional-order King Cobra system reduces to its classical chaotic form. The 3D phase plot presented in Figure 1 is obtained for system parameters (a, b, c, d, h, k) = (8, 1, 5, -1, -5, -6) and initial conditions ($x(0)$, $y(0)$, $z(0)$) = [0.1, 1, 0.1]. The attractor exhibits a typical chaotic structure characterized by non-periodic oscillations and sensitive dependence on initial conditions. The system parameter a is selected as the bifurcation parameter, while the other system parameters and initial conditions are kept unchanged throughout the analysis.

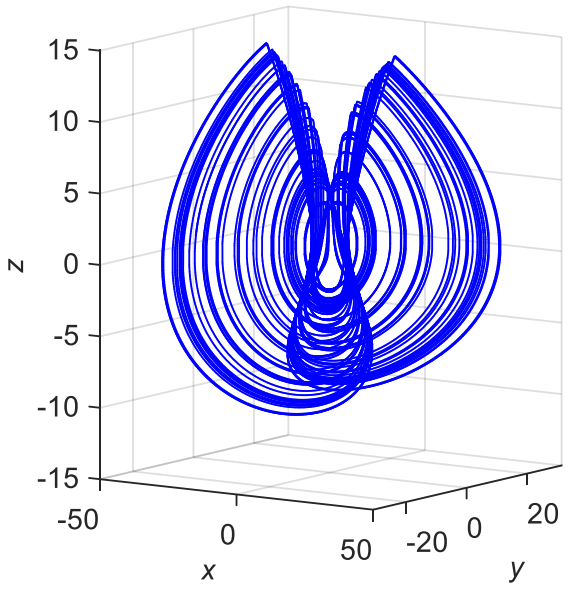
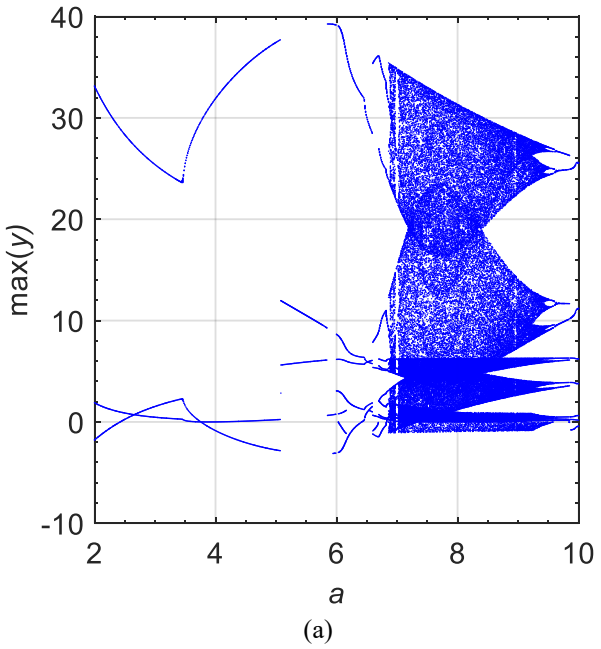
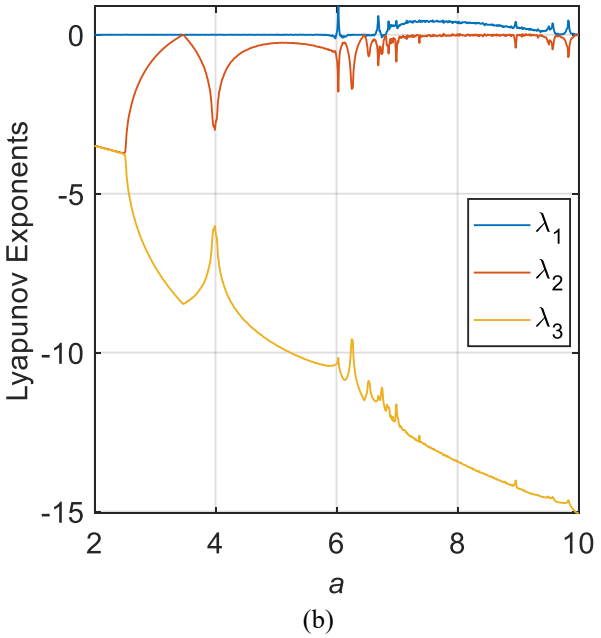


Figure 1. 3D phase plot of the integer-order King Cobra Chaotic system with parameters (a, b, c, d, h, k)=(8, 1, 5, -1, -5, -6) and initial conditions ($x(0)$, $y(0)$, $z(0)$) = [0.1, 1, 0.1].

For the conformable fractional-order case $\alpha = 0.95$, the dynamic behavior of the conformable King Cobra chaotic system is further investigated by varying the system parameter a within the range $2 < a < 10$. The bifurcation diagram shown in Figure 2(a) demonstrates a clear transition from periodic to chaotic motion as a increases, indicating strong parameter sensitivity. Correspondingly, the Lyapunov exponents plotted in Figure 2(b) confirm this transition, where the largest Lyapunov exponent becomes positive in the chaotic regions ($6.8 < a < 9.6$). These results verify the existence of chaotic behavior in the conformable fractional-order system and reveal that decreasing the fractional order slightly from unity ($\alpha = 1 \rightarrow 0.95$) maintains chaotic dynamics but alters the width and onset of chaotic intervals.



(a)



(b)

Figure 2. (a) Bifurcation diagram and (b) Lyapunov exponents of the conformable fractional-order King Cobra system for $\alpha = 0.95$ and $2 < a < 10$.

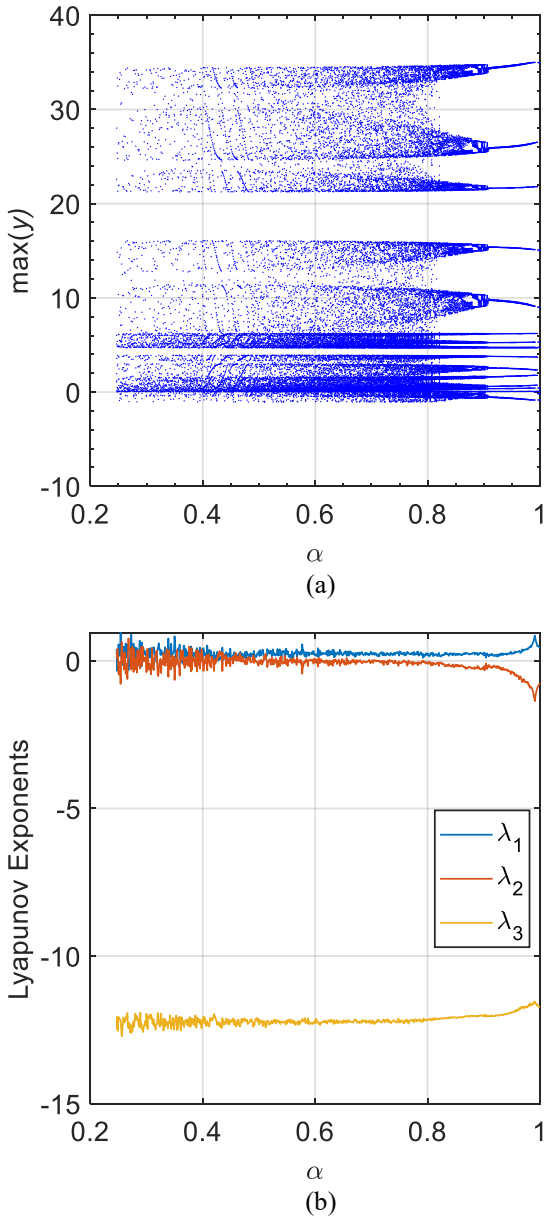


Figure 3. (a) Bifurcation diagram and (b) Lyapunov exponents of the conformable fractional-order King Cobra system for a=7 and $0.2 < \alpha < 1$.

For the next analysis, the system parameter is fixed at $a = 7$, and the fractional-order α is selected as the bifurcation parameter in the range $0.2 < \alpha < 1$. The corresponding bifurcation and Lyapunov exponents spectra are presented in Figure 3(a) and Figure 3(b), respectively. As observed in the bifurcation diagram, chaotic oscillations occur predominantly within the interval $0.2 < \alpha < 0.9$. However, the Lyapunov spectrum indicates that for $0.2 < \alpha < 0.4$, the first two Lyapunov exponents λ_1 and $\lambda_2$are unstable and do not simultaneously exhibit positive and zero values. It shows that true chaotic behavior may not be sustained in this region. Furthermore, for $0.9 < \alpha < 1$, the second Lyapunov exponent λ_2 becomes negative, which coincides with the bifurcation diagram and confirms that the system leaves the chaotic regime and transitions to periodic behavior as α approaches unity. These results highlight the strong influence of the conformable fractional order on the onset and disappearance of chaos in the conformable fractional-order King Cobra system.

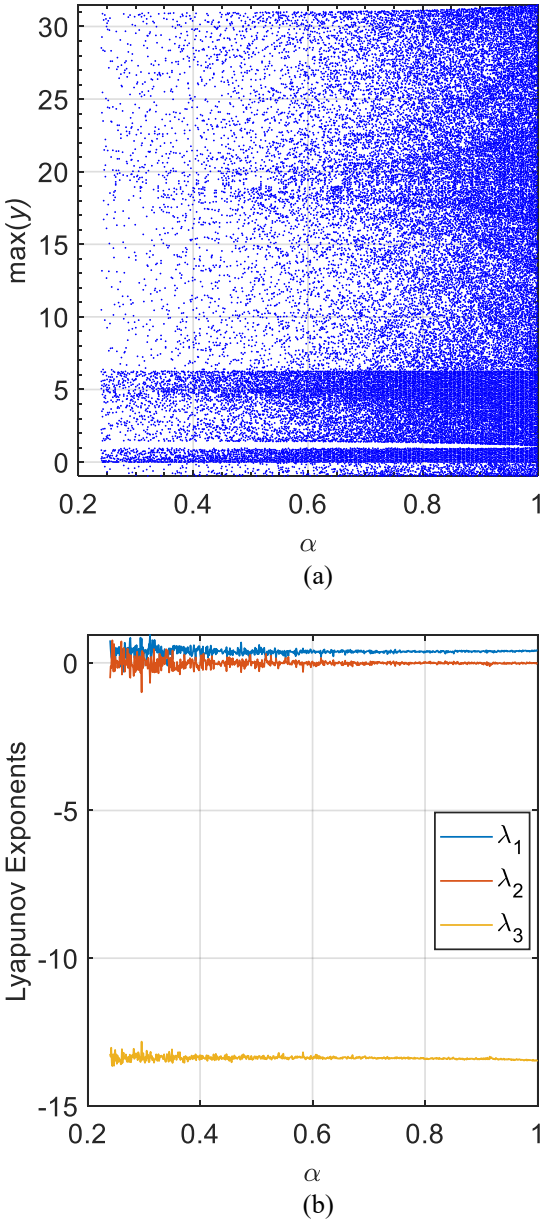


Figure 4. (a) Bifurcation diagram and (b) Lyapunov exponents of the conformable fractional-order King Cobra system for a=8 and $0.2 < \alpha < 1$.

To examine the combined influence of the system parameter a and the fractional order α on the dynamic behavior of the conformable fractional-order King Cobra chaotic system, phase portraits are presented in Figure 5(a–c) for different parameter combinations. In Figure 5(a), with a=8 and$\alpha = 0.5$, the attractor becomes more regular and less dispersed. When a is decreased to 7 while keeping $\alpha = 0.75$ (Figure 5 (b)), the attractor expands, and the trajectories become more scattered, such as an enhancement in chaotic intensity. Conversely, for a=8 and a higher fractional order of $\alpha = 0.95$ (Figure 5 (c)), the system exhibits a typical chaotic attractor with dense and irregular trajectories, indicating strong nonlinear interactions between the state variables. These results highlight that both the fractional order and the system parameter a significantly affect the complexity of the chaotic attractor.

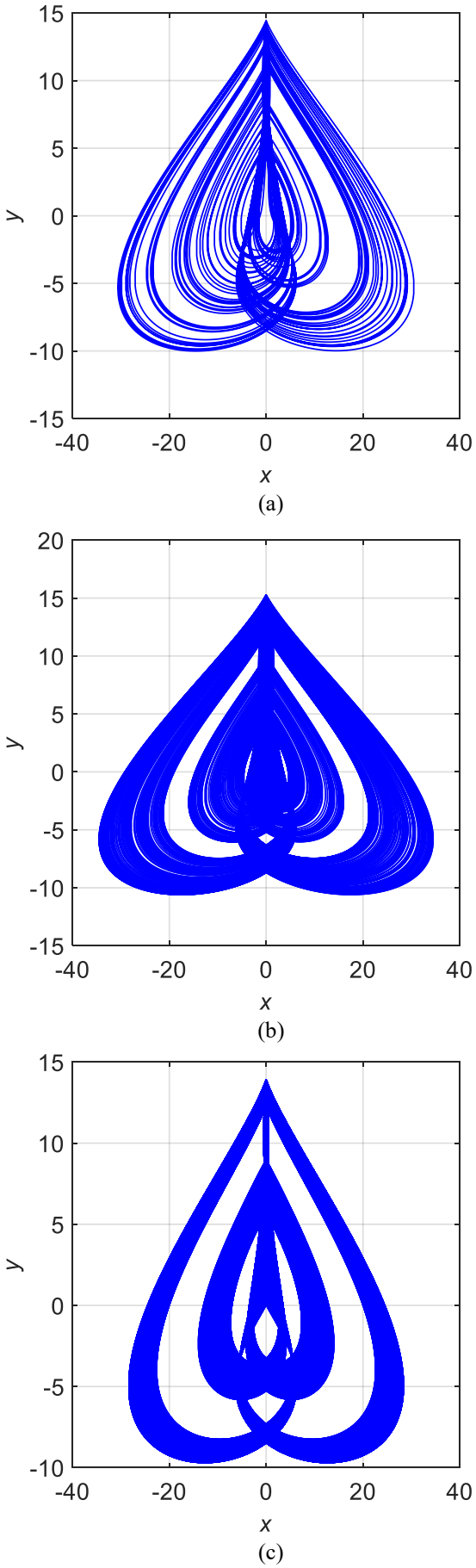


Figure 5. Phase portraits of conformable fractional-order King cobra chaotic system when (a) a=8, $\alpha = 0.5$, (b) a=7, $\alpha = 0.75$and (c) a=9, $\alpha = 0.95$.

3. SYNCHRONIZATION DESIGN VIA MULTI-STATE PI-ADRC CONTROL

3.1. Overview of the Control Framework

In order to achieve robust synchronization between the master and slave conformable fractional-order King Cobra chaotic systems, a multi-state PI-ADRC strategy is developed. Unlike traditional single-input control structures that inject the control signal only into one state equation, the proposed scheme applies independent control inputs to each state variable, i.e., $u = [u_1, u_2, u_3]^T$. This structure enables the controller to actively compensate for internal coupling, nonlinear interactions, and external disturbances acting on all states simultaneously.

Each subsystem of the slave chaotic system is equipped with a dedicated ESO, which estimates both the unmeasured states and the total disturbance dynamically. The control signal for each state is then generated based on a PI-type error feedback law combined with the ESO estimation, resulting in an adaptive, self-correcting control loop.

3.2. Mathematical Description of the Controller

The master system is expressed as:

$$T_\alpha(m_i) = f_i(m), i = 1,2,3, \tag{6}$$

and the slave system with control input becomes:

$$T_\alpha(s_i) = f(s) + \beta_i(u_i), i = 1,2,3 \tag{7}$$

where m and s are the states of the master and slave, respectively. The synchronization error is defined as:

$$e_i = s_i - m_i \tag{8}$$

For each subsystem, the ESO estimates the true states $\hat{s}_i$and the total disturbance $\hat{\partial}_i$ using [23]:

$$\begin{aligned} \dot{\hat{v}}_{1i} &= \hat{v}_{2i} + \delta_1(s_i - \hat{v}_{1i}) \\ \dot{\hat{v}}_{2i} &= \hat{v}_{3i} + \beta_i u_i + \delta_2(s_i - \hat{v}_{1i}) \\ \dot{\hat{v}}_{3i} &= \delta_3(s_i - \hat{v}_{1i}) \end{aligned} \tag{9}$$

where $\hat{v}_{1i} \approx s_i$ is the estimated output, $\hat{v}_{2i}$is the estimated derivative of the system output and $\hat{v}_{3i}$ represents the estimated total disturbance. The PI-based control law is given by:

$$u_i = \frac{1}{\beta_i}\left(-k_{p_i}e_i - k_{i_i}\int e_i dt - \hat{\partial}_i\right) \tag{10}$$

where $k_{p_i}$and k_{i_i} are the proportional and integral gains, respectively. Here, δ_i denotes the observer gain and $\beta_i$stands for the control input gain. The integral term ensures zero steady-state synchronization error, while the disturbance term $\hat{\partial}_i$ cancels out modeling uncertainties and nonlinear effects.

3.3. Stability Analysis

The closed-loop stability of the proposed multi-state PI-ADRC control scheme can be analyzed based on the error dynamics and the disturbance estimation capability of the Extended State Observer (ESO). Let the synchronization error be defined as in Eq. (8). The control law is designed in Eq. (10) such that the ESO estimates the total disturbance, including internal nonlinearities and external perturbations, and compensates for it in real time.

Under the assumption that the observer gains and controller parameters are properly selected, the estimation error of the ESO converges to a bounded neighborhood of zero. Consequently, the closed-loop error dynamics can be approximated by a stable linear system with proportional–integral feedback. According to standard ADRC theory, this structure ensures that the tracking errors e_i are uniformly ultimately bounded and converges asymptotically to zero.

Therefore, the proposed control system guarantees closed-loop stability in the sense of asymptotic synchronization. This conclusion is further supported by the simulation results in the next section, where all synchronization errors converge smoothly to zero without oscillation.

4. SIMULATION RESULTS

The control scheme is implemented in MATLAB using a conformable Euler-type integration method adapted for fractional-order derivatives. The master and slave systems are simulated simultaneously with conformable fractional order $\alpha = 0.75$and the time step $h_t = 10^{-3}$ with total simulation duration T=100 seconds. The system parameters are set to $a = 7$, $b = 1$, $c = 5$, $d = -1$, $h = -5$and $k = -6$. The initial conditions are selected as $m(0) = [0.1,1,0.1]$ and $s(0) = [0.1,0.5,0.1]$ to ensure distinct initial trajectories and emphasize synchronization behavior. The ESO parameters are set as $\delta = [862.65\ 2662.45\ 1]$ for all states, while the PI gains are tuned empirically as $K_p = [200\ 200\ 200]$ and $K_i = [115.65\ -0.90\ 1.42]$. All of the gains are determined by the Integral Time Absolute Error (ITAE)-based optimization algorithm to ensure fast convergence without inducing oscillations in the control inputs [24]. To evaluate the robustness of the proposed controller, random external disturbances are injected into the slave system dynamics in the form of additive Gaussian noise, modeled with the MATLAB function as '0.5*$rand$'. This perturbation simulates sensor noise and unmodeled environmental effects that typically occur in practical chaotic systems.

For numerical integration, the conformable derivative $T_\alpha f(t) = t^{\alpha-1} f'(t)$ is incorporated into the Euler update scheme, leading to the discrete-time formulation

$$x_{k+1} = x_k + h t_k^{\alpha-1} f(x_k) \tag{11}$$

where t_k denotes the simulation time at iteration k. This formulation enables efficient numerical implementation while preserving the conformable fractional-order dynamics.

Figure 6 illustrates the time-domain evolution of the master and slave system states under the proposed PI-ADRC synchronization strategy. It can be observed that, despite the fractional-order nature and different initial conditions of King Cobra system, the slave trajectories (red dashed lines) rapidly converge to those of the master system (blue solid lines) across all three states. This behavior confirms that the designed controller effectively compensates both internal nonlinearities and conformable derivative-induced dynamics. Steady-state synchronization is achieved within approximately t = 1 s that demonstrates the robustness and fast convergence capability of the multi-state PI-ADRC structure.

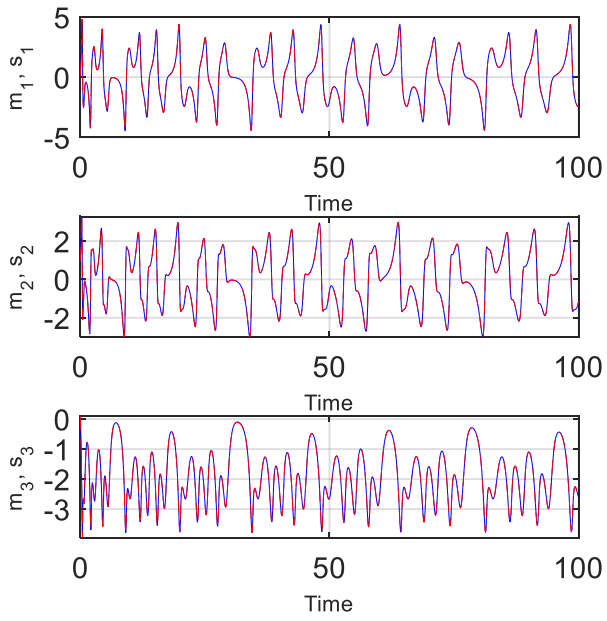


Figure 6. Time domain responses of the master (blue) and slave (red dashed) states under multi-state PI-ADRC synchronization.

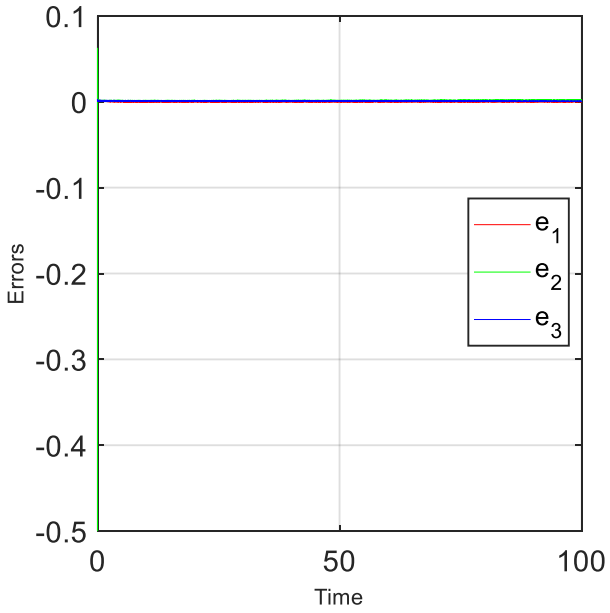


Figure 7. Synchronization error dynamics of the conformable fractional-order King Cobra chaotic system.

The synchronization errors are shown in Figure 7. The errors e_1, e_2, e_3 corresponding to each system state decay smoothly toward zero without oscillation, which validates the stability and accuracy of the designed control law. This confirms the effectiveness of the PI-ADRC approach in achieving stable and precise synchronization in conformable fractional-order chaotic systems.

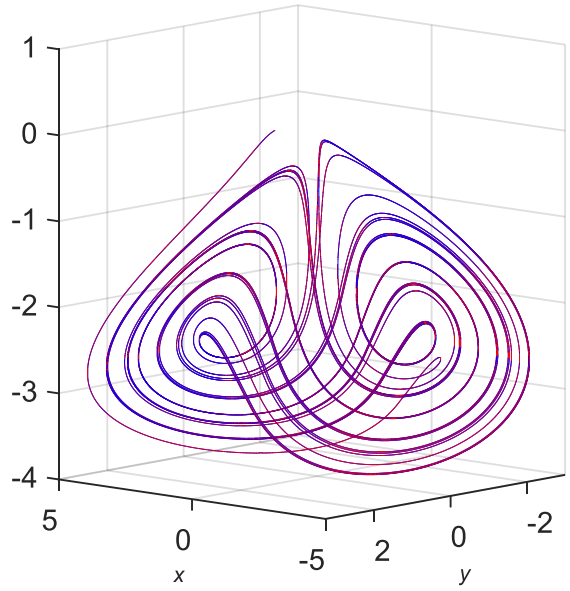


Figure 8. 3D Phase portrait of the synchronized master and slave systems.

The three-dimensional phase portrait of the master and slave systems is shown in Figure 8. The trajectories of the master (blue) and slave (red dashed) systems overlap completely after the transient period, indicating full synchronization in the state space. Initially, slight deviations are observed due to different initial conditions, but as time progresses, the controlled slave system precisely tracks the chaotic attractor of the master.

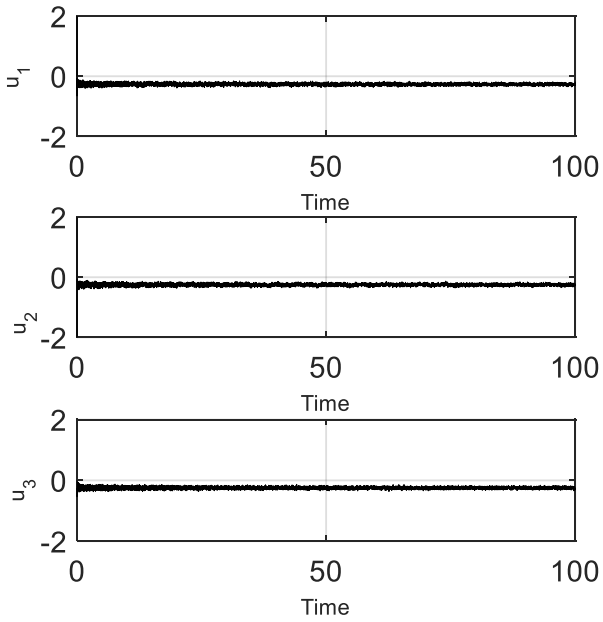


Figure 9. Control input signals u_1, u_2, u_3 generated by the multi-state PI-ADRC.

Figure 9 depicts the control input signals u_1, u_2, u_3 generated by the controller for each state. The control signals remain smooth and bounded, exhibiting no abrupt switching or chattering behavior. This demonstrates that the ADRC structure ensures robust yet energy-efficient control performance, even under nonlinear and fractional-order dynamics. The gradual stabilization of u_i further verifies that the ESO successfully isolates the disturbance components, enabling the PI-ADRC to focus solely on synchronization tracking.

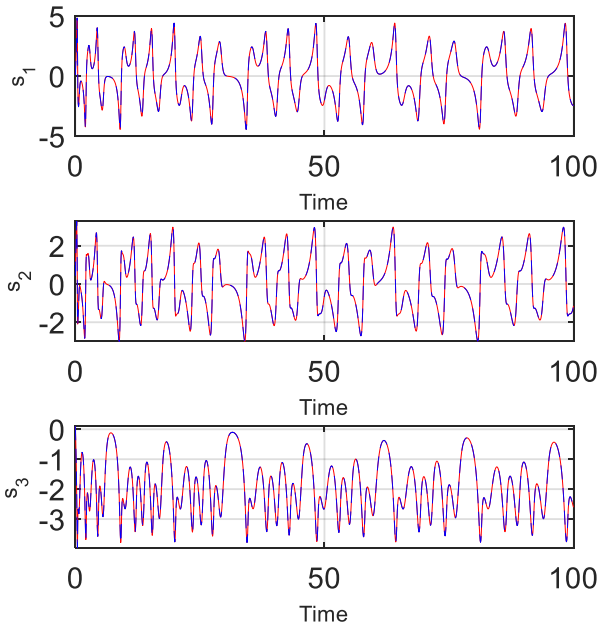


Figure 10. ESO estimated states $\hat{s}_i$compared with actual slave states s_i.

Figure 10 compares the actual slave system states $s_i$with their ESO-estimated counterparts $\hat{s}_i$. The estimation curves (blue dashed lines) almost perfectly coincide with the true system trajectories (red solid lines), which confirms that the designed observer effectively reconstructs the internal system dynamics in real time. This accurate state estimation allows the controller to respond adaptively to system variations and disturbances without explicit model knowledge, which is one of the main advantages of ADRC-based approach. Furthermore, Figure 11 presents the evolution of the estimated total disturbances $\hat{\partial}_i$ for all three states. It is observed that the disturbance estimates converge to stable bounded values, successfully capturing the unmodeled dynamics and compensating for them through the control channel. The simulation results clearly demonstrate that the proposed multi-state PI-ADRC controller achieves fast, accurate, and robust synchronization between two identical conformable fractional-order King Cobra chaotic systems. By simultaneously controlling all three states with independent adaptive observers, the structure enhances the estimation precision and significantly reduces synchronization errors.

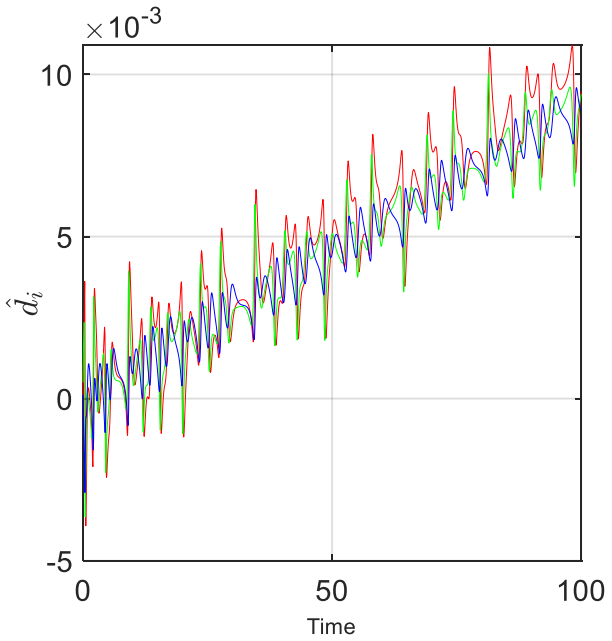


Figure 11. ESO disturbance estimations ($\hat{\partial}_i$) for each system state.

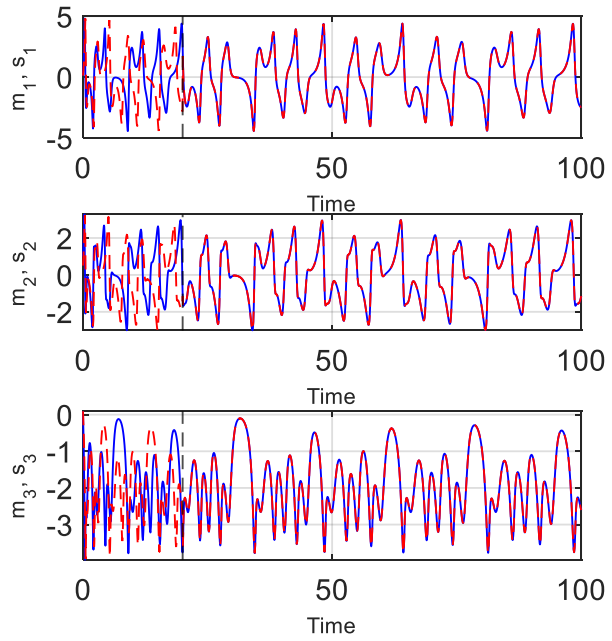


Figure 12. Time-domain responses of master and slave systems under switching control activation. The control input is inactive for t < 20 s and activated for t ≥ 20 s.

To demonstrate the effectiveness of the proposed control strategy, the controller is intentionally deactivated during the initial time interval (t < 20 s), allowing the slave system to evolve without control. As observed in Figure 12, the slave system fails to track the master system in this interval due to the inherent sensitivity of chaotic dynamics to initial conditions. At t = 20 s, the proposed multi-state PI-ADRC controller is activated. Following this activation, the slave system rapidly converges to the master system, and synchronization is achieved within a short time. This clear transition from unsynchronized to synchronized behavior highlights the effectiveness and robustness of the proposed control method.

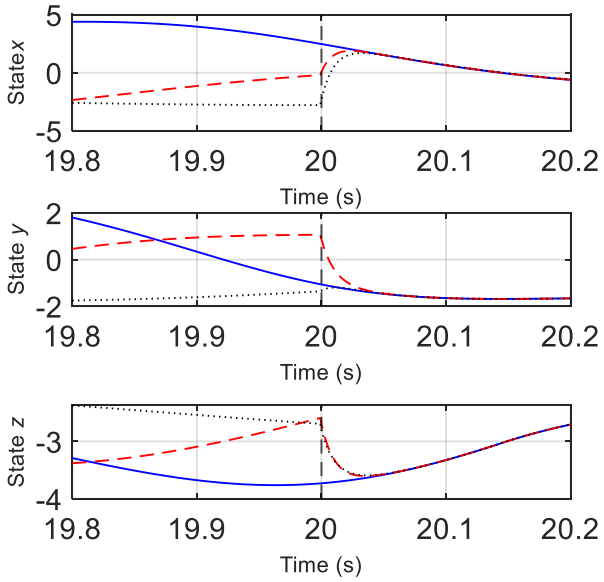


Figure 13. Comparison of synchronization performance of PI-ADRC and PID controllers under simultaneous activation at t = 20 s.

The comparative synchronization performance of the proposed PI-ADRC and the conventional PID controller is presented in Figure 13 around the controller activation instant. For t < 20 s, both controllers are inactive, and the slave systems evolve without synchronization. At t = 20 s, both controllers are activated simultaneously. It is observed that both control strategies are capable of achieving synchronization after activation; however, their performance differs across state variables. The PI-ADRC controller provides faster and smoother convergence particularly in the x state, whereas the PID controller shows relatively better transient behavior in the *y* state. For the *z* state, both methods exhibit similar synchronization performance. These results indicate that while both controllers are effective, the proposed PI-ADRC offers a more consistent and robust overall synchronization performance under the given conditions.

To further evaluate the robustness of the proposed control scheme, a sensitivity analysis was conducted by introducing a +10% variation in both the PI controller gains and the ESO parameters. In this scenario, the controller is first activated at t = 20 s using nominal parameters, and the gain variation is applied at t = 30 s. As shown in Figure 14, the synchronization performance is preserved even after the parameter perturbation. Although slight deviations in the transient response are observed following the variation, all state variables remain stable and continue to track the master system accurately. No instability or oscillatory divergence occurs. These results demonstrate that the proposed multi-state PI-ADRC framework does not require highly precise parameter tuning and exhibits strong robustness against moderate gain uncertainties.

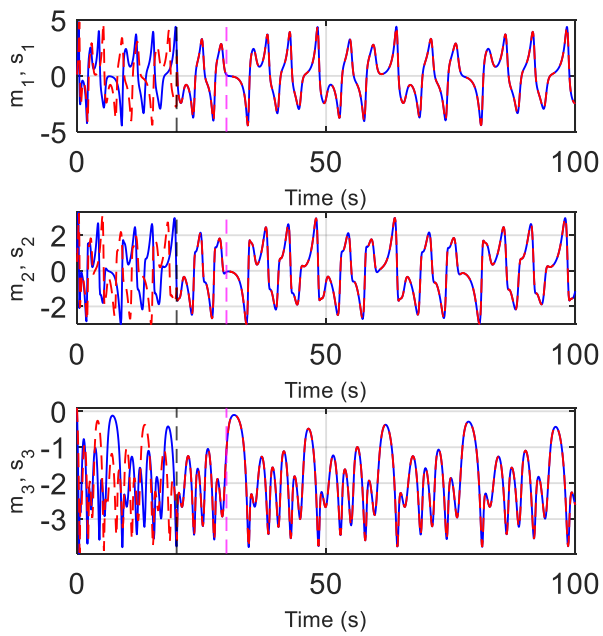


Figure 14. Robustness analysis of state responses under controller activation (t = 20 s) and +10% parameter variation applied at t = 30 s.

5. CONCLUSION AND DISCUSSION

In this study, the conformable fractional-order King Cobra chaotic system is investigated in detail, and its dynamic properties are analyzed through numerical simulations. By varying the fractional-order $\alpha$and the system parameter a, rich nonlinear behaviors are observed. The bifurcation and Lyapunov exponent analyses confirm the existence of chaos in certain parameter ranges, and demonstrated the sensitivity of the system to fractional-order variations. These findings emphasize the significant influence of conformable fractional calculus on the dynamical characteristics of chaotic systems.

Furthermore, a multi-state PI-ADRC strategy is designed and applied to achieve synchronization between two identical conformable King Cobra chaotic systems. The controller incorporated an ESO to estimate total disturbances and model uncertainties in real time. The numerical simulations verify that the proposed PI-ADRC successfully synchronized the slave system to the master system despite the presence of stochastic disturbances added to the slave dynamics. The synchronization errors converged rapidly to zero, and the ESO accurately tracked both system states and external disturbances, as illustrated in the simulation results. Compared to conventional control methods, the proposed PI-ADRC exhibits several advantages such as robustness against external noise, adaptability to nonlinear dynamics, and reduced sensitivity to modeling inaccuracies. These results confirm that the ADRC framework provides a powerful tool for synchronization control in chaotic systems.

In addition to synchronization control, the conformable fractional-order King Cobra system also has potential applications in smart systems such as secure communication and cryptographic signal processing. Owing to its high sensitivity to initial conditions and parameter variations, chaotic dynamics can be utilized for secure information masking and encryption schemes. The inclusion of the fractional-order parameter αintroduces an additional degree of freedom that enlarges the key space and enhances security flexibility. Moreover, the robust synchronization achieved through the proposed multi-state PI-ADRC framework enables reliable chaos-based communication between transmitter and receiver systems. Therefore, the presented approach may also contribute to the development of future smart and secure cyber-physical systems.

Conflict of Interest: No conflict of interest was declared by the authors.
Financial Disclosure: The authors declared that this study has received no financial support.

REFERENCES

[1] B. Emin, A. Akgul, F. Horasan, A. Gokyildirim, H. Calgan, and C. Volos, “Secure Encryption of Biomedical Images Based on Arneodo Chaotic System with the Lowest Fractional-Order Value,” Electronics, vol. 13, no. 11, p. 2122, 2024.

[2] E. N. Lorenz, “Deterministic Nonperiodic Flow,” J. Atmos. Sci., vol. 20, no. 2, pp. 130–141, 1963.

[3] G. Chen and T. Ueta, “Yet Another Chaotic Attractor,” Int. J. Bifurc. Chaos, vol. 09, no. 07, pp. 1465–1466, Jul. 1999, doi: 10.1142/S0218127499001024.

[4] A. Gokyildirim, Y. Uyaroglu, and I. Pehlivan, “A novel chaotic attractor and its weak signal detection application,” Optik (Stuttg)., vol. 127, no. 19, pp. 7889–7895, 2016, doi: 10.1016/j.ijleo.2016.05.150.

[5] S. Iqbal and J. Wang, “A novel fractional-order 3-D chaotic system and its application to secure communication based on chaos synchronization,” Phys. Scr., vol. 100, no. 2, p. 25243, 2025.

[6] B. Iskender Eroğlu, D. Avci, and N. Özdemir, “Optimal control problem for a conformable fractional heat conduction equation,” Acta Phys. Pol. A, vol. 132, no. 3, pp. 658–662, 2017.

[7] H. Nabil and H. Tayeb, “Fractional-order Modeling of Ecological Interactions with Hyperchaotic Dynamics for Secure Image Encryption,” Brazilian J. Phys., vol. 56, no. 3, p. 119, 2026.

[8] H. Calgan and M. Demirtas, “Design and implementation of fault tolerant fractional order controllers for the output power of self-excited induction generator,” Electr. Eng., vol. 103, no. 5, pp. 2373–2389, 2021.

[9] H. Nabil and H. Tayeb, “Fractional-order supply chain finance system with conformable derivative: Chaotic dynamics, complexity analysis, and RGB color image encryption,” J. Comput. Appl. Math., p. 117105, 2025.

[10] Y. Wang, “Dynamic analysis and synchronization of conformable fractional-order chaotic systems,” Eur. Phys. J. Plus, vol. 133, no. 11, p. 481, 2018.

[11] N. Das and S. Saha Ray, "Dynamical investigation of the perturbed Chen–Lee–Liu model with conformable fractional derivative," Zeitschrift für Naturforsch. A, vol. 79, no. 10, pp. 997–1010, 2024.

[12] D. Astekin and F. ADIGÜZEL, "Fractional-order adaptive terminal sliding mode control for synchronization of uncertain chaotic memristive Chua's circuit," Turkish J. Electr. Eng. Comput. Sci., vol. 33, no. 5, pp. 556–573, 2025.

[13] R. P. Chauhan, S. Kumar, S. Momani, and S. Hadid, "A dynamical study of the fractional order King Cobra model," in Computation and Modeling for Fractional Order Systems, Elsevier, 2024, pp. 135–154.

[14] H. Calgan and A. Gokyildirim, "Synchronization of Incommensurate Fractional-order King Cobra Chaotic System," Acad. Platf. J. Eng. Smart Syst., vol. 11, no. 3, pp. 184–190, 2023.

[15] N. A. Saeed, H. A. Saleh, W. A. El-Ganaini, M. Kamel, and M. S. Mohamed, "On a New Three-Dimensional Chaotic System with Adaptive Control and Chaos Synchronization," Shock Vib., vol. 2023, no. 1, p. 1969500, 2023.

[16] A. Gokyildirim, H. Calgan, and M. Demirtas, "Fractional-Order sliding mode control of a 4D memristive chaotic system," J. Vib. Control, vol. 30, no. 7–8, pp. 1604–1620, 2024.

[17] F. Adıgüzel, "An adaptive nonlinear controller design for a class of uncertain chaotic systems with single input using linear model reference," Chaos, Solitons & Fractals, vol. 199, p. 116683, 2025.

[18] A. Sun et al., "Application of model free active disturbance rejection controller in nuclear reactor power control," Prog. Nucl. Energy, vol. 140, p. 103907, 2021.

[19] J. Han, "From PID to active disturbance rejection control," IEEE Trans. Ind. Electron., vol. 56, no. 3, pp. 900–906, 2009.

[20] F. Doostdar and H. Mojallali, "An ADRC-based backstepping control design for a class of fractional-order systems," ISA Trans., vol. 121, pp. 140–146, 2022.

[21] E. Balcı, İ. Öztürk, and S. Kartal, "Dynamical behaviour of fractional order tumor model with Caputo and conformable fractional derivative," Chaos, Solitons & Fractals, vol. 123, pp. 43–51, 2019.

[22] P. Muthukumar, P. Balasubramaniam, and K. Ratnavelu, "Synchronization and an application of a novel fractional order King Cobra chaotic system," Chaos An Interdiscip. J. Nonlinear Sci., vol. 24, no. 3, 2014.

[23] X. Li, S. Wang, X. Wang, and T. Shi, "Permanent magnet brushless motor control based on ADRC," in MATEC Web of Conferences, EDP Sciences, 2016, p. 8003.

[24] A. Yesil, A. Gokyildirim, Y. Babacan, and H. Calgan, "A novel memristive chaotic jerk circuit and its microcontroller-based sliding mode control," J. Vib. Control, vol. 31, no. 17–18, pp. 3845–3864, 2025.